Accepted Manuscript

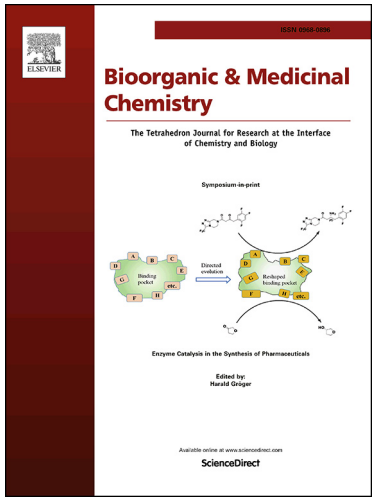

Medium Throughput Cage State Stability Screen of Conditions for the Generation of Gold Nanoparticles Encapsulated Within A Mini-Ferritin

T.A. Cornell, B.P. Orner

PII: S0968-0896(17)32341-6
DOI: https://doi.org/10.1016/j.bmc.2018.03.036
Reference: BMC 14274

To appear in: *Bioorganic & Medicinal Chemistry*

Received Date: 1 December 2017
Revised Date: 15 March 2018
Accepted Date: 23 March 2018

Please cite this article as: Cornell, T.A., Orner, B.P., Medium Throughput Cage State Stability Screen of Conditions for the Generation of Gold Nanoparticles Encapsulated Within A Mini-Ferritin, *Bioorganic & Medicinal Chemistry* (2018), doi: https://doi.org/10.1016/j.bmc.2018.03.036

Medium Throughput Cage State Stability Screen of Conditions for the Generation of Gold Nanoparticles Encapsulated Within A Mini-Ferritin

T. A. Cornell,[a], [b] and B. P. Orner*[a], [c]

[a] Research Conducted at Department of Chemistry
King's College London
London, United Kingdom
[b] Current Address: Dr. Thomas A. Cornell, Centre for Biomimetic Sensor Science, School of Materials Science and Engineering,
Nanyang Technological University, Singapore
[c] Current Address: Dr. Brendan P. Orner, 15 Robin Road Singapore
*Corresponding author. E-mail address: brendan.patrick.orner@gmail.com

Keywords: Protein-protein interactions • Nanoparticles • Protein design • Protein cages • Ferritins

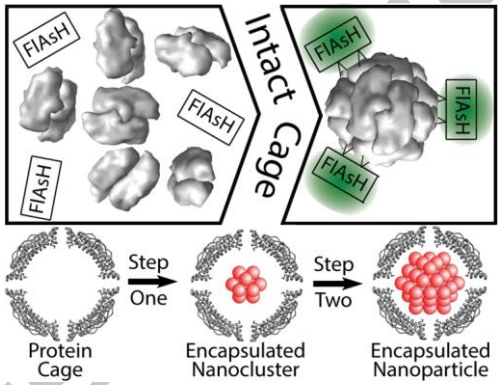

Abstract: Methods for the generation of nanoparticles encapsulated within cage proteins, such as ferritins, provide particles with low polydispersities due to size constraint by the cage. The proteins can provide enhanced water solubility to enable biological applications and affinity and identification tags to facilitate delivery or the assembly of advanced materials. Many effective methods have been developed, however, they are often impeded by cage protein instability in the presence of reagents or conditions for formation of the nanoparticles. Although the stability of ferritin cage quaternary structure can be enhanced, application of ferritins to materials science remains limited by unpredictable behaviour. Recently, we reported a medium throughput technique to directly detect the ferritin cage state. Herein, we expand this strategy to screen conditions commonly used for the formation of gold nanoparticles. Not only do we report nanoparticle formation conditions that permit ferritin stability, we establish a general screening strategy based on protein cage stability that could be applied to other protein cages or for the generation of other types of particles.

1. Introduction

As a close symbiosis between protein and material science research matures,[1,2] it is realized that the functionalization of nanomaterials with bio-

molecules not only enhances the properties of the materials, but can also assist their development for biological applications.[3,4] Toward these ends, nanocage proteins,[5] because of their hollow cavities with defined size and shape, have been used as size-constrained reactors to afford nanoparticles with narrow polydispersities.[6,7,8,9] In addition, they provide the resulting encapsulated particles with enhanced solubility, protect the particles from aggregating, and enable the further manipulation of the particles through bioconjugate and fusion strategies.[10,11]

While other nanocages, such as cowpea chlorotic mottle virus[6] or lumazine synthase,[12] have been used for nanoparticle formation, the well-characterised structure, unique size and symmetry, and native mineralisation activity of ferritins make them especially ideal for these applications, and, to date, gold,[13,14] silver,[15] copper,[16] cadmium,[17] palladium[18] and platinum[19] nanoparticles have been generated inside proteins of the ferritin family. Most ferritins assemble into nano-scale, spherical nanocages which act to maintain cellular iron homeostasis,[20,21,22,23,24] and the ferritin superfamily has provided excellent models for the study of protein quaternary structure[25,26,27,28,29,30] due to their relativity simple four-helix bundle-based monomer structures. Much ferritin-based materials research focuses on the mammalian horse spleen ferritin,[2,13,31,32] specifically, the non-catalytically active Light Chain (L-chain HsFn). This ferritin is a maxi-ferritin, assembling into a protein cage made up of twenty-four monomers, possessing octahedral symmetry, and having cavity and outer diameters of 9 and 11 nm, respectively.

Previously, we published a method for the generation of gold nanoparticles, which have been shown to be useful as catalysts, as contrast enhancing optical sensors and for medical diagnosis,[33] inside unmodified HsFn using a two-step reduction strategy (Figure 1B and Table S1).[13] The first step in the method involves the loading of gold ions into the ferritin cavity. Because the diffusion is slow, the solution can be rapidly desalted to remove gold external to the protein, a step that prevents gold precipitation on the outside of the cage.[11] Then the internalized gold is clustered with a fast reducing agent, $NaBH_4$, trapping it inside the nanocage. More gold feedstock is added, and the reaction mixture is then treated with a reducing agent, ascorbate, that requires a nucleating seed, resulting in slow growth of the nanocluster into a particle restricted to the size of the ferritin inner cavity. This method generates ferritin-encapsulated gold nanoparticles with extremely narrow polydispersities. However, follow-on attempts to establish this method as a general technique have been met with some difficulties.

As a first attempt to expand our methodology to other ferritins, we targeted the *E. coli* mini-ferritin, DNA binding protein from starved cells (**Dps**),[34,35] because, as a 12-meric, tetrahedral cage protein with a 9 nm outer diameter and 4.5 nm diameter cavity,[36,37] it should template gold nanoparticles of a size distinct from those we previously produced in the mammalian maxi-ferritin and it is expected that these smaller particles will have modified properties.[33,38,39] However, these attempts proved challenging due to both protein aggregation (see Figures 1C-top and S6B) and the protracted two day procedure, the length of which inhibits expeditious optimization. Therefore, we thought that the development of a strategy to rapidly and directly screen nanoparticle formation conditions with respect to protein cage stability would support the optimization process.

Previously, we reported an assay that allows for the robust and selective detection of protein cage assembly in complex conditions, such as cellular lysates,[40, 41] and we have recently expanded it to the screening of protein libraries in living cells.[42] This assay was built upon work developed by the Tsien[43, 44] and Schepartz[45,46] labs and employs the bisarsinical probe, FlAsH, that fluoresces once its two ethanedithiol (EDT) ligands are replaced by four sulphur atoms projected from cysteine residues engineered in an ideal relative geometry across a protein-protein interface. To detect Dps mini-ferritin cages over other oligomerization states, we designed cage-specific FlAsH binding sites as pairs of cysteines fused to the Dps monomer C-terminus by a small peptide spacer (ProAlaGly) resulting in the protein, **DpsPAGCC.** Importantly, this method detects the cage over other states, including aggregate, and we have described its application in medium throughput format with 96-well plates to probe the stability of **DpsPAGCC** while scanning various pH and denaturation conditions simultaneously.[40,41]

Herein, we present the evolution of this medium throughput, protein cage stability assay, to screen conditions typically used for the generation of gold nanoparticles.[13] Because of the generality of the strategy's design, it is thought that, in principle, it could be easily ported to other protein cages and conditions for the generation of other types of nanoparticles.

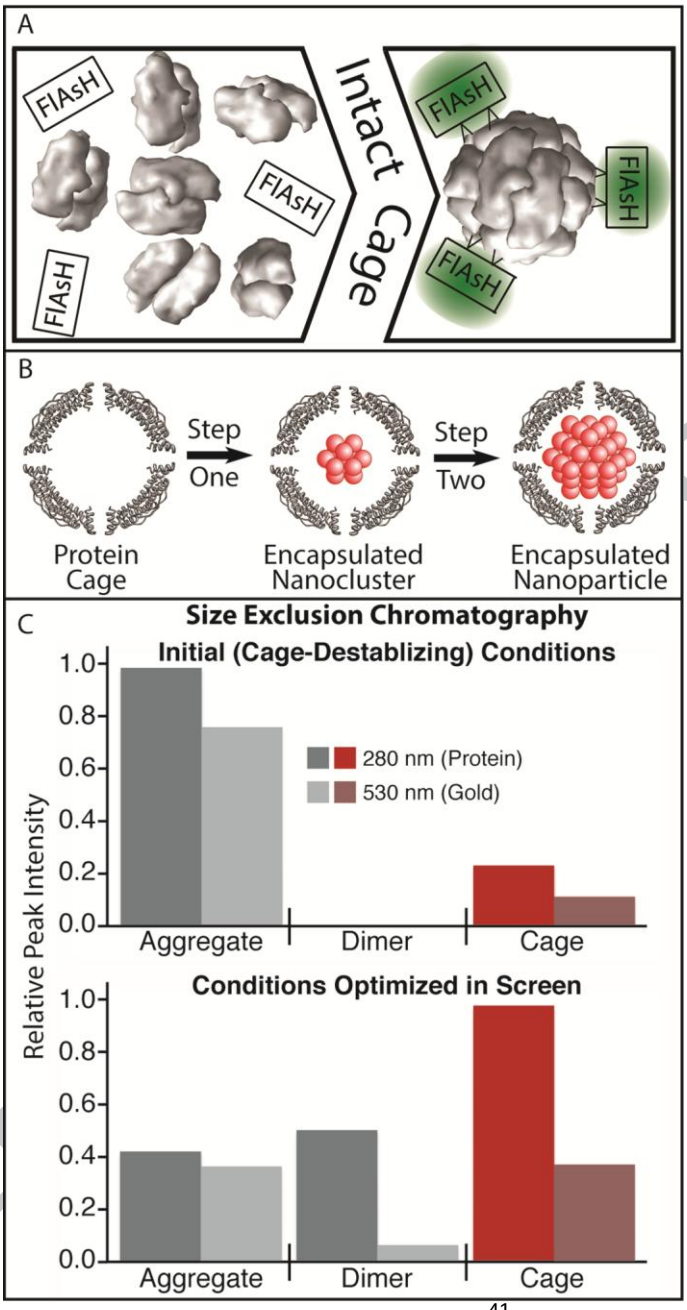

Figure 1. (A) The medium throughput assay[41] employs the fluorophore FlAsH[43] and an optimized, cage-specific binding site to directly detect the cage state in ferritin proteins. (B) A two step reduction strategy[13] was used to generate gold nanoparticles inside horse spleen maxi-ferritin protein cages. These original conditions were optimized to favour stable **Dps** mini-ferritin protein cages through the medium throughput assay described herein. (C) Relative maximal absorbance for size exclusion chromatographic analysis of **Dps** stability and gold association (top) after exposure to nanoparticle generation conditions originally developed for horse spleen ferritin,[13] and (bottom) after exposure to nanoparticle generation conditions optimised for **Dps** through the medium throughput screen for protein cage stability described herein. The samples were monitored at 280 nm (dark bars) to observe protein and at 530 nm (light bars) to monitor gold, and the cage state is highlighted (red bars) Experimental details and conditions are provided and compared below in Table S1.

2. Results and Discussion

At the initiation of this project, we determined the effect the conditions we previously used for the generation of gold nanoparticles inside HsFn[13] have on the quaternary structure of **Dps.** While expressed and purified **Dps** (see below and supporting information for full experimental details and characterization data) typically shows a major peak corresponding to intact protein nanocage when subjected to size exclusion chromatography (SEC) analysis (Fig. S6A), **Dps** exposed to the original nanoparticle formation conditions, resulted in primarily the formation of large protein (280 nm) aggregates with associated gold (520nm) (Figures 1C-top and S6B) indicating that the conditions that worked well for HsFn cause cage instability and disassembly in **Dps**.

Traditionally, optimization of these conditions would be conducted through trial and error, which is a time- and resource-consuming process. Instead, we applied our previously published, medium throughput, 96-well format technique for the detection of mini-ferritin quaternary structure (see above).[40,41] This techniques relies on detection of key protein-protein interactions, that are diagnostic of the assembled cage state, through the engineering of assembly-dependent binding sites for the reagent FlAsH for which binding is required to generate a fluorescent signal (Figure 1A). Thus, increased signal correlates to an increase in population of the cage state. This technique is robust and has been applied to a 96-well plate format. In this case, **Dps** was engineered to present these binding sites, resulting in the protein **DpsPAGCC**. The goal of this research is to probe the cage-state stability of **DpsPAGCC** using the 96-well plate assay in conditions commonly used for the generation of gold nanoparticles (Figure 2-lower right) for the purpose of shifting the aggregate to the cage population of **Dps** from the ratio observed in our initial “cage-destabilizing” conditions (Figure 1C-top) to conditions that favour the cage (Figure 1C-bottom).

Expressed and purified **DpsPAGCC** (see below and supporting information for full experimental details and characterization data) was subjected to varying concentrations of reagents which are commonly used for the generation of gold nanoparticles inside ferritins ($HAuCl_4$, $NaBH_4$, $NaCNBH_3$, trisodium citrate, ascorbic acid)[13,14] (Figure 2). Moreover, to determine if any observed instability was due to pH changes caused by the reagents, these conditions were screened both in unbuffered and buffered (100 mM Tris.HCl, 100 mM NaCl, 1 mM EDTA, pH 7.8) solution. It was felt this information, albeit limited, could help shed some preliminary light on mechanism and direct future optimization while maintaining the spirit of a rapid assay with advanced throughput. These conditions were screened in 96-well format in order to increase throughput and ensure reproducible comparison of data (Figure 2-bottom right). (Note: To aid comparison, the initial “cage-destabilizing conditions used for Figure 1C-top are highlighted with black arrows in Figure 2 and the optimized conditions used for Figure 1C-bottom are highlighted with red arrows.)

The protein cage state of the mini-ferritin, as detected by the assay, was observed to be remarkably sensitive to the various conditions. Sodium cyanoborohydride and trisodium citrate conditions maintained stable protein

nanocages across a wide range of concentrations with citrate demonstrating a slight stabilizing effect in unbuffered water. Ascorbic acid induced destabilization only at high concentration in buffer, but an effect on stability was extremely pronounced when not buffered. Interestingly, the cage state is quite sensitive to chloroauric acid, the gold source, but buffered conditions can extend the stability through a window of concentrations that does provide some flexibility. Interestingly, sodium borohydride, the reductant we initially used successfully with HsFn, destabilizes the mini-ferritin cage even in buffered conditions although, curiously, it appears to have a stabilizing effect at low concentrations in unbuffered water. The comparison between sodium borohydride and sodium cyanoborohydride is striking with an almost complete loss of structure with borohydride but stability across the concentration range with cyanoborohydride. Along with confirming the observation that the conditions that had been successful with HsFn caused major cage destabilization in **Dps** (Figure 1C-top), the screen also suggests a way forward, thereby emphasizing the utility and power of the strategy.

Because the assay allowed the screening of multiple conditions simultaneously, we were able to generate sufficient information to make a multi-step optimization where we decreased the concentration of the gold solution to avoid local concentration effects, swapped the first reductant from sodium borohydride to sodium cyanoborohydride, and buffered all solutions using Tris. Convincingly, chromatographic analysis of **Dps** subjected to these new conditions demonstrated much less protein aggregation, and intact cages (280 nm) with associated gold (530 nm) made up the major population (Fig. 1C-bottom and Fig. S6C). Thus, these results suggested that the optimized conditions were more compatible with stability of the protein cage and that the screening method was capable in identifying these conditions.

It should be noted that this research is meant to establish a proof of principle to expand the medium throughput protein stability screen in novel directions and to demonstrate that it can be used to optimize conditions for the generation of nanoparticles inside protein cages. While this goal has been achieved as evidenced by the data presented in this report, the conditions should in no way be considered conclusive. Although the stability of the mini-protein has been greatly improved, further optimizations could be imagined and it would be expected that screening additional buffers, a wider range of pH or other gold sources could prove beneficial.

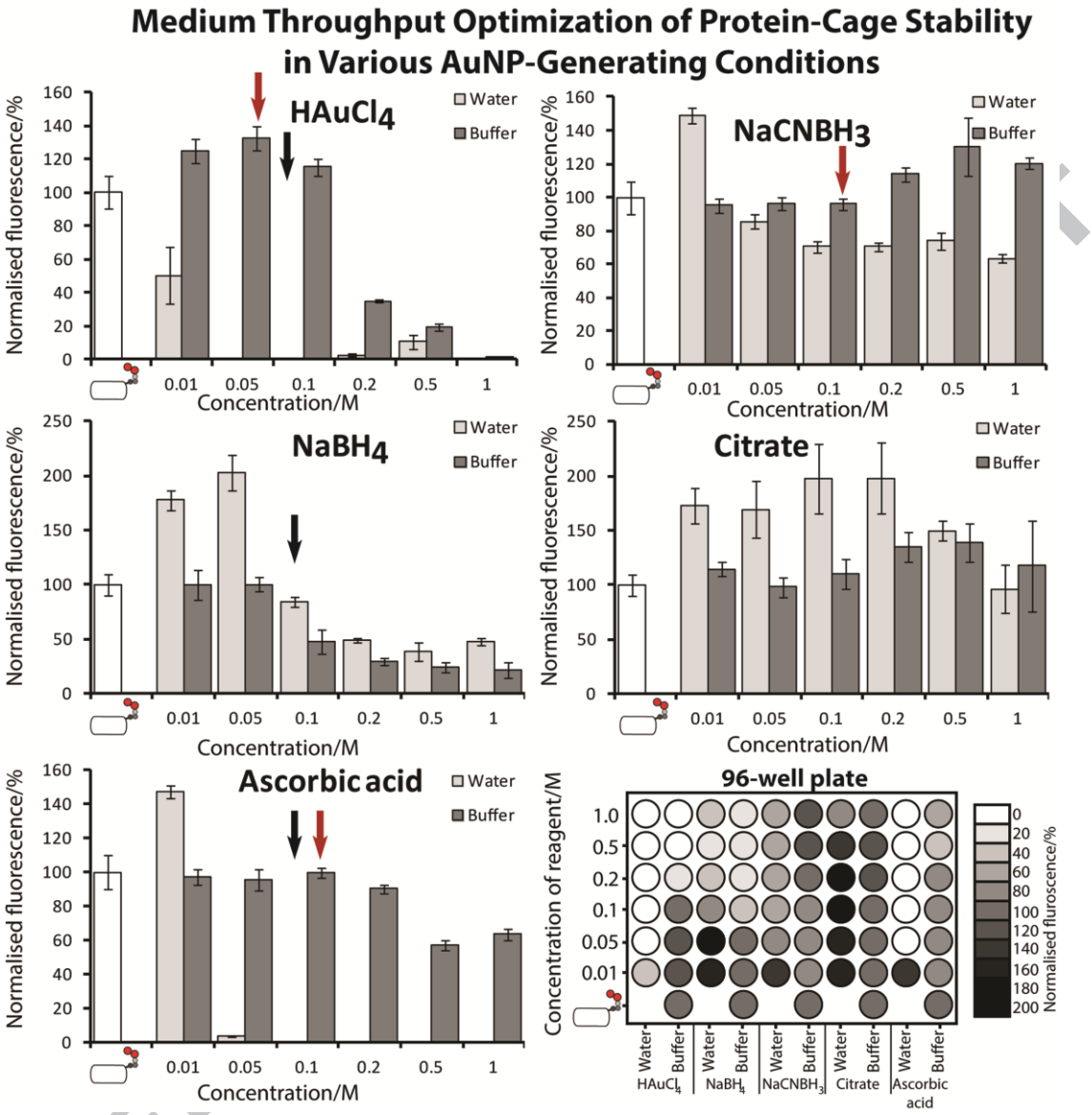

Figure 2. Medium throughput protein stability screen of conditions for the generation of gold nanoparticles encapsulated within the mini-ferritin protein cage, **DpsPAGCC**. An assay was used that correlates fluorescence with the formation of key 3-fold symmetric protein-protein interactions in the mini-ferritin in the presence of (top left) chloroauric acid (top right), sodium cyanoborohydride (middle left), sodium borohydride (middle right), trisodium citrate (bottom left), and ascorbic acid in both buffer (dark grey) and unbuffered (light grey) conditions. A schematic of a 96-well plate (Bottom right) with greyscale corresponding to average fluorescence intensity used in the bar graphs is presented. The data is normalised to **DpsPAGCC** in buffer with no added reagents (white bar). All data is averaged from 3 replicates. Arrows indicate conditions used for Figure 1C (black –conditions applied to **DpsPACC** from Fan *et al*. (2010)[13] originally used for the generation of gold nanoparticles inside horse spleen ferritin (HsFn), Red – conditions optimized through this screen) and the schematized protein represents **DpSPAGCC** where the circles indicate the FlAsH binding site (black-Pro, dark grey-Ala,

light grey-Gly, red-Cys). See Supporting Information for comparison of conditions. Error bars are S.D.

4. Conclusions

In this report, we have described an application of our medium throughput assay for the cage state of ferritin proteins. This method is based on the direct detection of the formation of designed FlAsH binding sites at symmetry-related protein-protein interfaces.[41] We used the technique to screen conditions for the formation of gold nanoparticles inside the mini-ferritin, **Dps**, and to determine if they are compatible with protein stability. While providing initial optimization for the type of nanoparticles of our immediate interest (gold nanoparticles) using our specific protein cage (a mini-ferritin), it further demonstrates the flexibility and practical utility of our protein cage stability assay which we are applying to the high throughput screening of protein libraries[42] and to understand the fundamentals of protein assembly. More generally, this strategy could be very easily and directly expanded to screen a wider range of conditions, conditions for the generation of other types of nanoparticles, or conditions that are optimized for other protein cages.

5. Experimental Details

The supporting information contains SDS-PAGE and sequencing data from the purification of **Dps** and **DpsPAGCC**, SEC of purified **DpsPAGCC,** sequences of transfer primers, SEC chromatograms of the data used to generate Figure 1C, and comparisons of initial and optimized nanoparticle formation conditions.

5.1 Cloning and expression of Dps and DpsPAGCC

The gene for **Dps** in the plasmid pET-32b was expressed and purified as previously described.[47] In short, the vector containing the gene coding for wild type **Dps** (see Fig. S5 for full sequence) was electroporated into BL21 *E.coli* cells and plated on LB plates (50 µl/ml carbenicillin). Selected colonies were then grown in LB (5 ml, 37 °C, overnight) as a pre-culture which was later added to LB (500 ml) and grown (37 °C) until an $O.D_{600}$ of 0.6 was reached. Protein expression was then induced by the addition of IPTG (final concentration 400 mM) and the cultures were further incubated (3 h, 30 °C). The cells were isolated by centrifugation (10,000 rpm, 20 min, 4 °C). The cell pellet was resuspended with lysis buffer (50 mM NaH_2PO_4, 300 mM NaCl, 40 mM Imidazole, pH 8) and sonicated (15 min with 10 s on/off pulses, Sonics Vibra Cell). The protein solutions were clarified by centrifugation (10,000 rpm, 20 min, 4 °C) and then filtered (Pall, 0.2 µm). **Dps** was purified via affinity chromatography through a His-6 tag by means of a GE 5 ml Histrap FF Column using wash buffer (30 mM NaH_2PO_4, 300 mM NaCl, 40 mM Imidazole, pH 7.6). The protein was eluted using elution buffer (30 mM $NaHPO_4$, 300 mM NaCl, 500 mM Imidazole, pH 7.6) and then digested with enterokinase (NEB, 2 µg/ml) to remove the affinity tag. The digestion reaction was followed by a second Histrap (GE, Histrap FF, 5 ml, (wash buffer-40 mM Imidazole, 50 mM NaH_2PO_4, 300 mM NaCl, pH 7.4), (elution buffer-500 mM

Imidazole, 50 mM NaH_2PO_4, 300 mM NaCl, pH 7.4)) to remove the tag from solution. The protein solutions were further purified by gel filtration chromatography (GE Hiload 16/60 Superdex with running buffer (50 mM Tris.HCl, 50 mM NaCl, pH 7.8.)). The degree of purification was assessed with SDS PAGE (see Fig. S1) and SEC (see Fig. S6A).

The design for **DpsPAGCC**, was established in previously published work.[41] The gene was transferred from pET-32b to pET-46 to reduce the size of the affinity tag. The construct was amplified from the pET-32b plasmid with primers providing ligation independent cloning (LIC) sites (Figure S4). The PCR solution included Pfu reaction buffer (Promega, 5 µl of 10x), dNTP mix (Fermentas, 2 µl of a solution containing dATP, dTTP, dGTP, and dCTP at 2 mM each), forward and reverse primers (400 ng each, Integrated DNA technologies, see Figure S4 for primer sequences), the template (100 ng) and Pfu polymerase (Promega, 2 µl of 2.5 U/ µl) in 50 µl total volume and was subjected to an initial melting step (95 °C for 30 s), followed by 30 cycles of amplification (95 °C for 30 s, 55 °C for 45 s and 72 °C for 1 min) followed by 72 °C for 7 min. The resulting PCR product was isolated by gel purification (Qiagen). The PCR product was then treated with T4 polymerase to create complementary overhangs (NEB buffer 2, 2 µl of 10x buffer), dATP (NEB, 2 µl of 25 mM), DTT (Sigma, 1 µl of 100 mM), BSA (NEB, 0.2 µl of 100x), PCR product (0.3 pmol) and T4 DNA polymerase (NEB, 0.6 µl of 10 U/µl) in a total volume of 20 µl, 30 min, 22 °C). The insert was annealed to the opened plasmid (0.5 µl of plasmid solution (50 ng/µl)) by incubating (room temperature, 30 min) followed by a second incubation with EDTA (room temperature, 30 min, 1 µl of 100 mM). The constructs (2.5 µl) were transformed (XL-1 Blue, Novagen) and the resulting colonies were assessed by colony PCR. A solution of Gotaq reaction buffer (5 µl of 5x), dNTP mix (Promega, 2 µl of a solution containing dATP, dTTP, dGTP, and dCTP at 2 mM each), T7 promoter and terminator primers (150 ng each, Eurofins MWG), Gotaq DNA polymerase (Promega, 0.25 µl of 5 U/ µl), colony suspension (10 µl of a 50 µl total colony suspension in deionised water) and deionised water (5 µl), was subjected to an initial melting step (95 °C for 10 min) followed by amplification 30 cycles (95 °C for 30 s, 59 °C for 30 s and 72 °C for 30 s followed by 72 °C for 7 min) Clones demonstrating a PCR product of the predicted size were subjected to miniprep (Promega) and the resulting purified plasmid was sequenced (see Fig. S5 for full sequence).

The vector containing **DpsPAGCC** was transformed into Rosetta *E.coli* cells (Novagen) and plated on LB agar plates (50 µl/ml of carbenicillin and 34 µl/ml of chloramphenicol). Selected colonies were then grown in LB (5 ml, 37 °C, overnight) as a pre-culture which was added to LB (500 ml) and grown (37 °C) until an $O.D_{600}$ of 0.6. Protein expression was then induced by the addition of IPTG (250 µl of a 1 M stock) and the cultures were further incubated (3 h, 30 °C). The cells were isolated by centrifugation (4,000 rpm, 20 min, 4 °C). The cell pellet was resuspended in lysis buffer (50 mM NaH_2PO_4, 300 mM NaCl, 40 mM Imidazole, 1 mM EDTA, pH 8). Cellytic (10x, Sigma) was added and the solution was incubated (20 min, on ice) and then sonicated (Misonix, ultrasonic cell distruptor, and pulsed for for 5 min (5 s on, 5 s off)). The protein solution was clarified by centrifugation (15,000 rpm, 45 min at 4 °C) and then filtered (Sartorius, 0.2 µm). **DpsPAGCC** was purified via affinity purification (GE, Histrap FF, 5 ml, (wash buffer-40 mM Imidazole, 50

mM NaH_2PO_4, 300 mM NaCl, pH 7.4), (elution buffer-500 mM Imidazole, 50 mM NaH_2PO_4, 300 mM NaCl, pH 7.4)), followed by gel filtration chromatography (GE Hiload 16/60 Superdex, running buffer- FlAsH buffer (100 mM Tris.HCl, 100 mM NaCl, 1 mM EDTA, pH 7.8). The degree of purification was assessed with SDS PAGE (see Figure S2) and SEC (see Figure S3).

5.2 Protein cage stability screen of DpsPAGCC with reagents for gold nanocage formation

A medium throughput assay based on our previous work[41,40] was performed using **DpsPAGCC**. The protein (final concentration 0.1 mg/ml) was incubated in FlAsH buffer (100 mM Tris.HCl, 100 mM NaCl, 1 mM EDTA, pH 7.8) in the presence of the various reagents in a total volume of 200 µl. Each reagent (chloroauric acid, sodium borohydride, sodium cyanoborohydride, trisodium citrate and ascorbic acid, all sourced from Sigma) were solubilised in either water (followed by no pH adjustment) or FlAsH buffer (followed by pH adjustment to 7.8 if necessary). The reagents were added to each well with varying final concentrations (0.01 M, 0.05 M, 0.1 M, 0.2 M, 0.5 M and 1 M) and the solutions were incubated (1 h, room temperature). To these solutions TCEP (Sigma, final concentration of 3.5 mM in FlAsH buffer), EDT (Sigma, final concentration of 1 mM in FlAsH buffer) and 2-ME (Sigma, final concentration of 1 mM in FlAsH buffer) were added, the resulting solutions were incubated (2 h, room temperature), after which FlAsH-EDT_2 (Invitrogen, final concentration of 0.1 µM, 2 h, room temperature) was added and the resulting solutions were further incubated. Each sample was prepared directly in a black Corning 96 well plate which was scanned in a PerkinElmer Envision 2101 Multilabel plate reader (Ex filter 485 nm bandwidth 14 nm, Em filter 535 nm bandwidth 25 nm). Each sample was prepared three times separately and each plate was reread three times and averaged.

5.3 Conditions for the formation of nanoparticles inside HsFn from Fan *et al.* (2010)[13] applied to Dps (Conditions used for Figures 1C-top and S6B)

Following the original method for the generation of nanoparticles in HsFn as previously described,[13] the initial gold source (22.6 µl of 0.1 M $HAuCl_4$ solution in water) was added to the protein, **Dps**, **(**1 ml of a 1 mg/ml, in phosphate buffer, 50 mM Na_2PO_4, 100 mM NaCl, pH 7). This solution was incubated (3 h, room temp) and then the sample was desalted (GE 5 ml HiTrap desalting column, into Tris buffer (50 mM Tris, 50 mM NaCl, pH 7.8)) to remove any un-encapsulated gold. The protein was collected (1 ml) and the first reducing agent was added (20 µl of 0.1 M $NaBH_4$ solubilised in water) and the resulting solution was incubated (3 h, room temp) with shaking. After initial reduction, a second gold solution was added (10 µl of a 0.1 M $HAuCl_4$ solubilised in water) followed by a second reducing agent (30 µl of 0.1 M ascorbic acid solubilised in water) followed by incubation (overnight, room temp). Samples were centrifuged (10 min, 10,000 rpm) before SEC characterisation.

5.4 Conditions optimized in this report through the medium throughput assay applied to Dps (Conditions used for Fig. 1C-bottom and Fig. S6C)

The first gold source (100 µl of 0.05 mM $HAuCl_4$ in Tris buffer (50 mM Tris.HCl, pH 7.8)) was added to 1 ml of 1 mg/ml of **Dps** (in 50 mM Tris.HCl, pH 7.8), and the solution was incubated (2 h, room temp). This sample was desalted using a GE 5 ml HiTrap desalting column and Tris buffer (50 mM Tris, 50 mM NaCl, pH 7.8) to remove any un-encapsulated gold. The protein peak was collected (1 ml) and the first reducing agent was added (100 µl of 0.1 M $NaCNBH_3$ in Tris buffer (50 mM Tris.HCl, pH 7.8)) and the solution was incubated (3 h, room temp) with shaking. After incubation, a second gold solution was added (100 µl of 0.05 mM $HAuCl_4$ in Tris buffer (50 mM Tris.HCl, pH 7.8)), as well as a second reducing agent (50 µl of 0.1 mM ascorbic acid in Tris buffer (50 mM Tris.HCl, pH 7.8)) and this was incubated (overnight, room temperature) before SEC characterisation.

5.5 Size exclusion chromatography (SEC)

The samples (0.5 mg/ml) in Tris buffer (50 mM Tris.HCl, 50 mM NaCl, pH 7.8) were injected (0.5 ml) on to a size exclusion column (GE Superdex 200 10/300 GL) at 0.5 ml/min. All samples were analysed for both protein stability (280 nm) and associated nanoparticle formation (520 nm).

Acknowledgements

We thank N. Luedtke, M. Peczuh, Y. Zhang, and M. Ardejani for insightful conversations, and R. Fan for the plasmid coding for WT Dps in pET-32b. We also thank D. Thurston's lab for help and access to instrumentation and an anonymous reviewer from a previous submission for suggestions to improve the manuscript. T.A.C was sponsored by a BSE scholarship at King's. The research was supported by a Marie Curie CIG: PCIG13-GA-2013-618538, and BPO's personal salary.

References

[1] Whitesides, G. M.; Grzybowski, B. *Science* **2002**, *295*, 2418.
[2] Uchida, M.; Klem, M. T. ; Allen, M.; Suci, P.; Flenniken, M.; Gillitzer, E.; Varpness, Z.; Liepold, L. O.; Young, M.; Douglas, T. *Adv. Mater.* **2007**, *19*, 1025.
[3] Uchida, M.; Flenniken, M. L.; Allen, M.; Willits, D. A.; Crowley, B. E.; Brumfield S.; Willis, A. F.; Jackiw, L.; Jutila, M.; Young, M. J.; Douglas, T. *J. Am. Chem. Soc.* **2006**, *128*, 16626.
[4] Bhaskar, S.; Lim S. *NPG Asia Materials* **2017***, 9*, e371.
[5] Zhang, Y.; Ardejani, M.S.; Orner, B. P. *Chem. Asian J.* **2016***, 11*, 2814.
[6] Zschoche, R.; Hilvert, D. *J. Am. Chem. Soc*. **2015**, *137*, 16121.
[7] Abe, S.; Maity, B.; Ueno, T. *Chem. Commun.* **2013***, 52,* 6496.
[8] Douglas, T.; Young, M. *Nature* **1998**, *393*, 152.
[9] Klem, M. T.; Willits, D.; Solis, D. J.; Belcher, A. M.; Young, M.; Douglas, T. *Adv. Funct. Mater.* **2005**, *15*, 1489.

[10] Butts, C. A.; Swift, J.; Kang, S.; Di Constanzo, L.; Christianson, D. W.; Saven, J. G.; Dmochowski, I. J. *Biochemistry* **2008**, *47*, 12729.
[11] Zhang, L.; Swift, J.; Butts, C. A .; Yerubandi, C. A .; Dmochowski, I. J.; *J.Inorg. Biochem.* **2007**, *101*, 1719.
[12] Shenton, W.; Mann, S.; Colfen, H.; Bacher, A.; Fischer, M. *Angew. Chem.* **2001**, *40*, 442.
[13] Fan, R.; Chew, S. W.; Cheong, V. V.; Orner, B. P. *Small* **2010***, 6*, 1483.
[14] Keyes, J. D.; Hilton, R. J.; Farrer, J.; Watt, R. K. *J. Nanopart. Res.* **2011**, *13*, 2563.
[15] Kramer, R. M.; Li, C.; Carter, D. C.; Stone, M. O.; Naik, R. R. *J. Am. Chem. Soc.* **2004**, *126*, 13282.
[16] Galvez, N.; Sanchez, P.; Dominguez-Vera, J. M. *Dalt.Trans.* **2005**, 2492.
[17] Yamashita, I.; Hayashi, J.; Hara, M. *Chem. Lett.* **2004**, *33*, 1158.
[18] Ueno, T.; Suzuki, M.; Goto, T.; Matsumoto, T.; Nagayama, K.; Wantanabe, Y. *Angew. Chem.* **2004**, *43*, 2527.
[19] Zhang, L.; Laug, L.; Munchgesang, W.; Pippel, E.; Gosele, U.; Brandsch, M.; Knez, M. *Nano Lett.* **2010**, *10*, 219.
[20] Aisen, P.; Listowsky, I. *Annu. Rev. Biochem.* **1980**, *49*, 357.
[21] Theil, E. C. *Annu. Rev. Biochem.* **1987**, *56*, 289.
[22] Theil, E. C.; Tosha, T.; Behera, R. K. *Acc. Chem. Res.* **2016***, 49*, 784.
[23] Pulsipher, K. W.; Dmochowski, I. J. *Isr. J. Chem.* **2016***, 56*, 660.
[24] Zhang, Y.; Orner, B. P. *Int. J. Mol. Sci.* **2011***, 12*, 5406.
[25] Huard, D. J. E.; Kane, K. M.; Tezcan, F. A. *Nat. Chem. Biol.* **2013** *9*, 169.
[26] Zhang, Y.; Raudah, S.; Teo, H.; Teo, G. W. S.; Fan, R.; Sun, X.; Orner, B. P. *J. Biol. Chem.* **2010**, *285*, 12078.
[27] Ardejani, M. S.; Li, N. X.; Orner, B. P. *Biochemistry,* **2011***, 50*, 4029.
[28] Ardejani, M. S.; Chok, X. L.; Foo, C. J.; Orner, B. P. *Chem. Commun.* **2013**, *49*, 3528.
[29] Zhang, Y.; Wang, L.; Ardejani, M. S.; Aris, N. F.; Li, X.; Orner, B. P.; Wang, F. *J. Biochem.* **2015**, 158, 505.
[30] Cornell, T. A.; Srivastava, Y.; Jauch, R.; Fan, R.; Orner, B. P. *Biochemistry* **2017***, 56*, 3894.
[31] Granier, T.; Gallois, B.; Dautant, A.; D'Estaintot, B. L.; Precigoux, G. *Acta Crystall.* **1997**, *D53*, 580.
[32] de Val, N.; Declercq, J. P.; Lim, C. K.; Crichton, R. R. *J. Inorg. Biochem.* **2012**, *112*, 77
[33] Daniel, M. C.; Astruc, D. *Chem. Rev.* **2004**, *104*, 293.
[34] Almiron, M.; Link, A. J.; Furlong, D.; Kolter, R. *Gen. Dev.* **1992**, *6*, 2646.
[35] Martinez, A.; Kolter, R. *J. Bact.* **1997**, *179*, 5188.
[36] Grant, R. A.; Filman, D. J.; Finkel, S. E.; Kolter, R.; Hogle, J. M. *Nat. Struct. Biol.* **1998**, *5*, 294.
[37] Zhang, Y.; Fu, J.; Chee, S. Y.; Ang, E. X. W.; Orner, B. P. *Protein Sci.* **2011**, *20*, 1907.
[38] Lin Q.; Sun, Z. *Opik* **2011**, *122*, 1031.
[39] Scholl, J. A.; Koh, A. L.; Dionne, J. A. *Nature* **2012**, *483*, 421.
[40] Cornell, T. A.; Orner, B. P. *Methods Mol. Biol., **2015**, 1252*, 79.
[41] Cornell, T. A.; Fu, J.; Newland, S. H.; Orner, B. P. *J. Am. Chem. Soc. **2013**, 135*, 16618.

[42] Cornell, T. A.; Ardejani, M. S.; Fu, J.; Newland, S. H.; Zhang, Y.; Orner, B. P. *Biochemistry* **2018**, *57*, 604.
[43] Griffin, B. A.; Adams, S. R.; Tsien, R. Y. *Science* **1998**, *281*, 269.
[44] Adams, S. R.; Campbell, R. E.; Gross, L. A.; Martin, B. R.; Walkup, G. K.; Yao, Y.; Llopis, J.; Tsien, R. Y. *J. Am. Chem. Soc.* **2002**, *124*, 6063.
[45] Luedtke, N.W.; Dexter, R.J.; Fried, D.B.; Schepartz, A. *Nat. Chem. Biol.* 2007, **3**, 779.
[46] Ray-Saha, S.; Schepartz, A. *Chembiochem* **2010**, *11*, 2089.
[47] Fan, R.; Boyle, A. L.; Vee, V. C.; See, L. N.; Orner, B. P. *Biochemistry* **2009,** *48,* 5623.